



university of
groningen

Investigation of the energy resolution of high purity germanium detectors using trapezoidal filtering

BACHELOR THESIS PROJECT

July 11, 2022

Author:

Koyo Yoshihara S3894886

Supervisors:

Dr. M.Kavatsyuk
prof. dr. Nasser Kalantar

Abstract

In order to compensate for the count losses experienced in standard pileups rejection methods, the trapezoidal filtering algorithm is implemented to detect the energy of two pulses when piled up together. Results showed that the full width at half maximum without pulse pileups equals 3.26 keV and 3.54 keV with pulse pileups where the pulse time separation is above 4000 nanoseconds. The trapezoidal algorithm consists of three steps: step filter function, moving average filter then the differentiation filter to correct for the ballistic deficits, noise induced high frequency signals and pulse pileups respectively. The algorithm analyzed 20000 waveforms randomly out of 111837 waveforms(each waveform spanning 5000 channels) where all events are artificially piled up for pulse time separations in the ranges of 3000 to 6000 nanoseconds.

Contents

1	Introduction	3
1.1	Motivation	3
1.2	High purity germanium(HPGe) detector	3
1.3	GAINS setup and GELINA facility	3
1.4	Pulse pileups	5
2	Research Aim	8
3	Set up and Experimental Method	8
3.1	Algorithm	8
3.1.1	Step Function Filter	8
3.1.2	Moving average filter	9
3.1.3	Differentiator	9
3.2	Hardware	11
3.2.1	Digitizer	11
3.2.2	Setup	11
3.3	Energy calibration	12
3.4	Data Processing	13
4	Results	15
4.1	Optimizing P and G values	15
4.2	Energy calibration	16
4.3	Relationship between mean energy/FWHM and pulse pileup delay	18
5	Discussion	21
5.1	Energy resolution	21
5.2	Peaking and gap time	21
5.3	Energy calibration	22
6	Conclusion	23
7	Appendix	26
7.1	FWHM and mean energy against pulse time separation values	26

1 Introduction

1.1 Motivation

Nuclear energy has been a feasible energy source amid the current energy crisis [1]. Not only it is a relatively clean energy source with fewer carbon footprints compared to fossil fuels, but it also is reliable and cost-effective [1]. Although there has been a significant amount of resistance towards the usage of nuclear energy due to incidents such as the Fukushima and Chernobyl accidents, with careful inspection and better development of the facilities, it can be deemed as an appropriate energy source [2].

The investigation of the neutron cross-section is essential for building reliable nuclear reactors as it allows the calculation of reactor cores. Thus, its performance depends largely on the accuracy of measuring these cross-sections [3]. There are broadly two types of neutron scattering reactions: elastic and inelastic neutron scattering. This report will only focus on the inelastic scattering of neutrons. Inelastic neutron scattering is an experimental technique used for exploring the atomic and molecular motions of a particle [4].

1.2 High purity germanium(HPGe) detector

The high purity germanium detector is an ideal detector to use in gamma and x-ray spectroscopy due to its relatively high resolution. These are mainly due to two reasons: its lower average energy necessary to create electron-hole pairs(3.6eV) and can be thicker(sensitive thickness of centimetres) compared to silicon. This allows absorption of higher energy photons [5].

However Germanium has a low bandgap of 0.7eV, which can lead to thermalization of photons with energies much larger than the band gap being absorbed causing recombinations which is undesirable since it can lead to the detectors heating up. Thermalisation gives rise to a drastic increase in noise due to large bulk currents induced. Hence germanium detectors are required to be cooled down to (77.2 K) so that only electrons which are excited by the gamma-rays can cross the bandgap [6].

HPGe detectors produce the highest resolution commercially available in recent years. They are highly useful for measuring radiation. Situations include medical applications, radiometric assay, nuclear security and nuclear plant safety [5].

1.3 GAINS setup and GELINA facility

The GELINA(Gamma array for inelastic neutron scattering) facility is a Neutron Time-of-Flight Facility which consists of a high-power pulsed linear electron accelerator, a post-accelerating beam compression magnet system, a mercury-cooled uranium target, and flight paths with measurement equipment [7]. As shown in figure 1 electron from the linear accelerator hits the Uranium target that acts as a neutron source, which then produces a Bremsstrahlung radiation. Bremsstrahlung radiation is defined as the deceleration of electrons when another electron collides with it while producing gamma rays[8]. These gamma-rays interact with Uranium

through (γ, xn) and $(\gamma, \text{fission})$ reactions, thus releasing neutrons. These neutrons are then scattered from a sample, producing gamma-rays which are then detected by the HPGe (high purity Germanium detector). These are known as the neutron-induced events and they are of main interest in this report [7]. The data is then analysed through the digitizer.

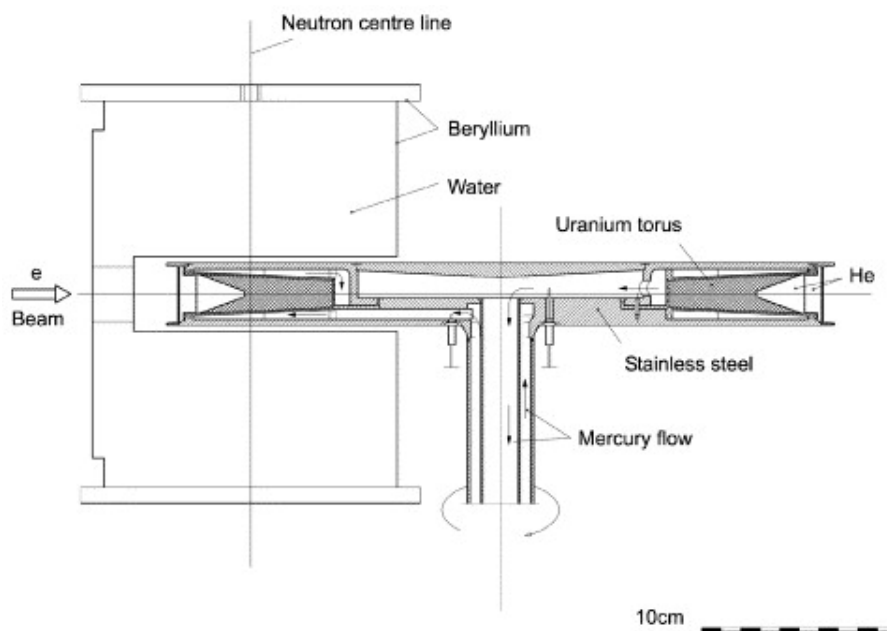


Figure 1: Schematic diagram of the GELINA facility before the accelerated electrons colliding with Uranium. Note that the main purpose of this image is to explain how the electrons collide with Uranium, other features such as mercury flow or Beryllium etc are not relevant thus are not explained. Image extracted from [9]

The GAINS (Gamma Array for Inelastic Neutron Scattering) setup composes of two or four HPGe detectors and a classical acquisition system [10]. The GAINS spectrometer which consists of 12 HPGe detectors placed at 125° , 110° and 150° with respect to the beam direction, is installed at 200 metres away from the Uranium source as shown in figure 2 [10].



Figure 2: GAINS setup. Image extracted from [10]

1.4 Pulse pileups

Pulse pileups are when two pulses overlap and an addition of their respective amplitudes occur. This happens when the HPGe detector detects two gamma rays in a single event due to the two gamma rays apart during its arrival is closer than its detectors resolution [11]. An image of a pulse pileup is shown below in figure 3.

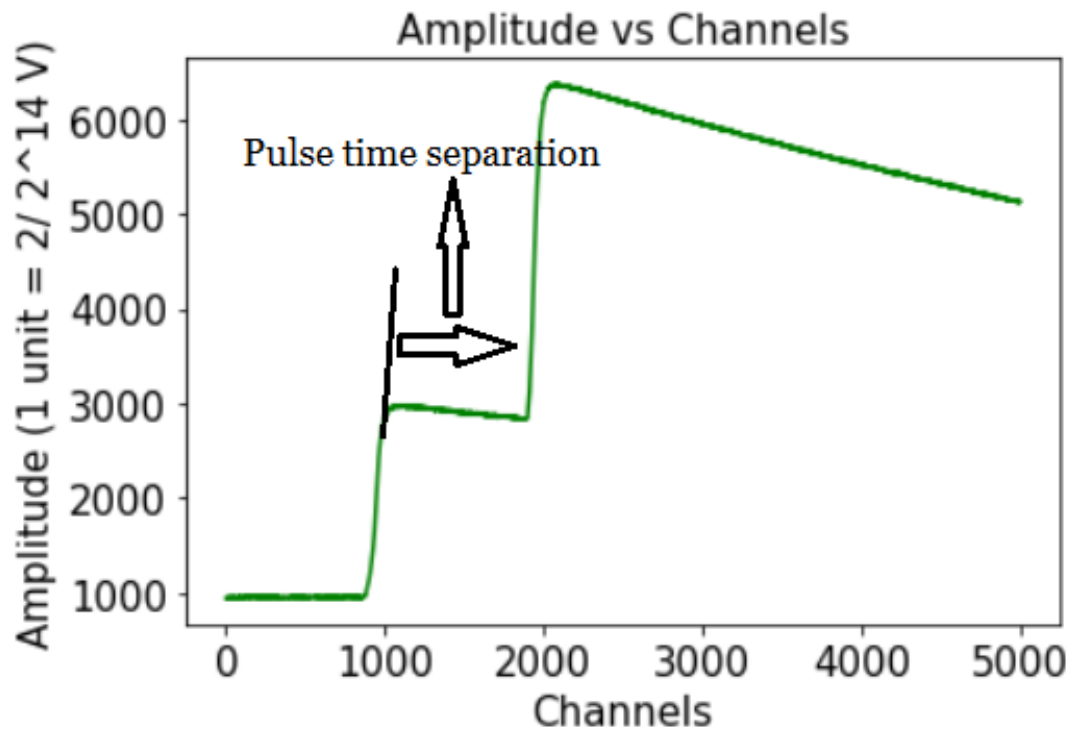


Figure 3: Pulse pileup for one of the raw signals. The two pulses are separated by a certain pulse time separation

The main issue with pulse pileups are that it causes distortions of the energy spectrum as the detector records the sum of the amplitudes of the two pulses instead of recording both amplitudes distinctively. As a result, the spectrum will end up having less counts at the intended energy level, additionally, a peak will appear higher up due to the sum of the two amplitudes as shown below in figure 5.

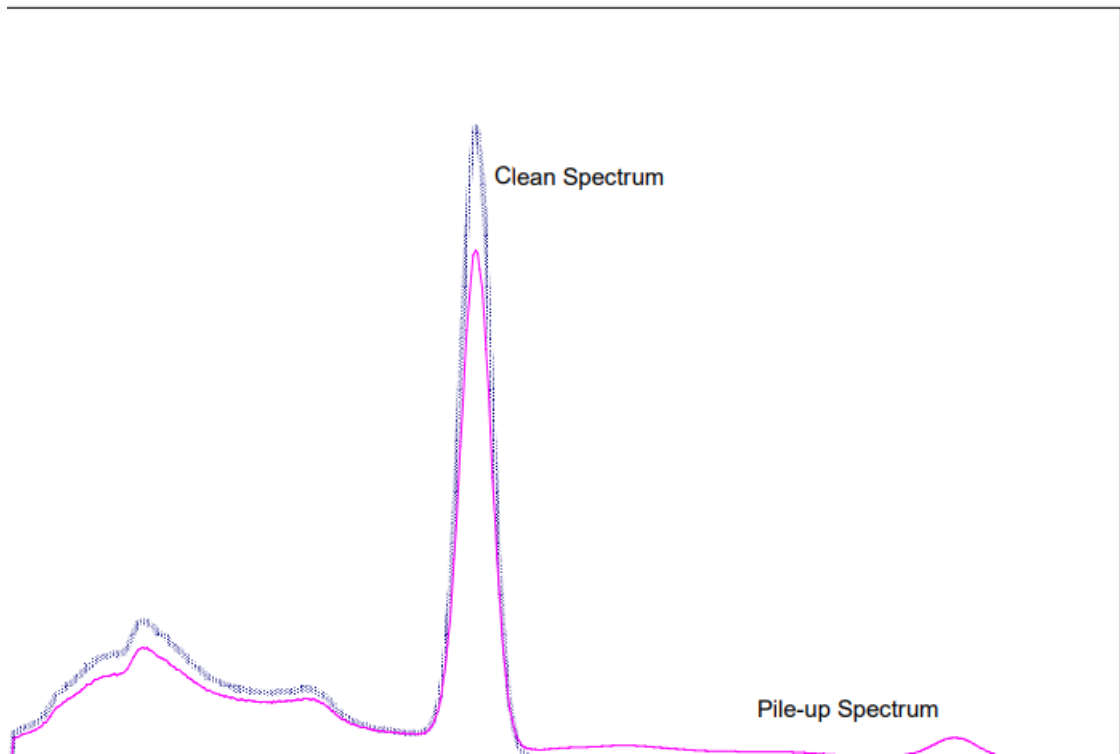


Figure 4: Comparison of the energy spectrum with and without pulse pileups. Image extracted from [11].

A common mitigation measure done to avoid pulse pileups are known as pileup rejection. This is when all events which include pulse pileups are rejected and not included in the energy spectrum [11]. However as a consequence, it ends up having significant reductions in counts which implies that it requires a longer measurement duration to collect sufficient data. This is not ideal as it is time consuming and reducing its thus not being efficient. To tackle this issue, this paper aims to resolve this issue by introducing the trapezoidal filtering algorithm with the intention to detect two pulse amplitudes in the presence of a pulse pileup event. More details will be included in the research aim section.

This report will mainly be focusing on the neutron-induced gamma-rays for the sake of investigating the relationship between the energy resolution and the pileups using digital pulse processing(DPP).

2 Research Aim

The research aim is phrased as follows: Detecting both pulse heights in the event of a pulse pileup event. This allows accurate determination of the actual pulse amplitude or voltage of each gamma ray. For this reason, all events included pulses which were artificially piled up to test if using the trapezoidal filtering algorithm is able to produce an energy spectrum without any distortions. This was done by selecting two waveforms randomly and adding on top of each other. The parameters which are used to define the distortions in an energy spectrum are: Full width at half maximum(FWHM) and the mean energy(peak position) of the 1173.3 keV peak assuming that the peak is fitted with a gaussian.

3 Set up and Experimental Method

3.1 Algorithm

The three main aspects which affect the detector's efficiency are : pileups, ballistic effects and signal to noise ratio.

There are three main algorithms which are used to improve the detector's energy: Step function filter, moving average filter and the differentiator.

3.1.1 Step Function Filter

The step function filter corrects for the loss of ballistic deficits. Ballistic deficits are when the pulses experiences a loss in output or amplitude after it has risen to its peak [12]. In order for accurate calculations of the pulse amplitude, the unnecessary loss of output must be corrected using the step function filter as shown in the figure below:

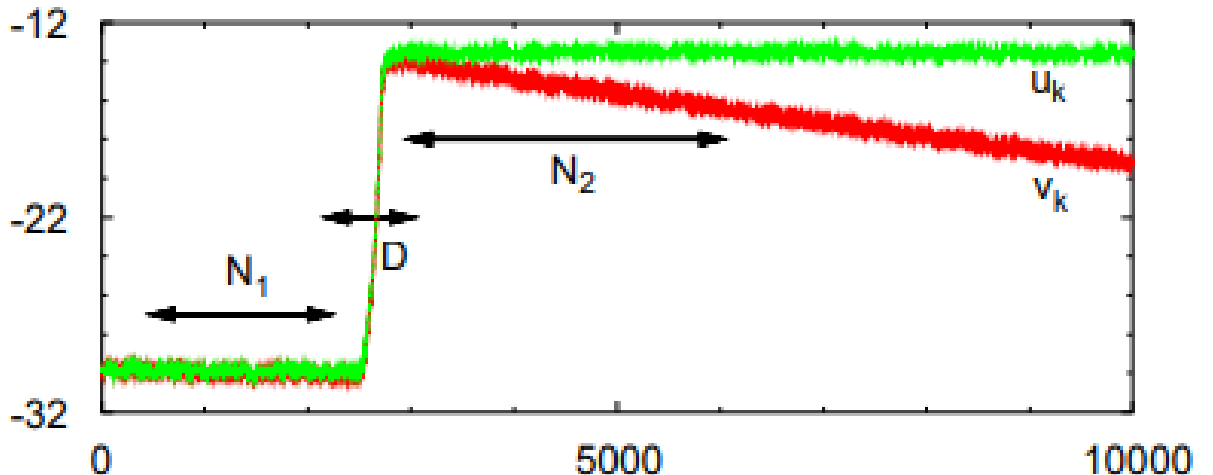


Figure 5: The pulse shape before(red) and after(green) the implementation of the step function filter. D: rising time and $N_1 = N_2 =$ time interval before and after rise. Image extracted from [7].

The step function filter corrects for the ballistic deficits by first extracting the decay constant(τ) by fitting the pole zero cancellation to the decaying region of the pulse [13] [7]. The pole zero coefficient is:

$$\beta = e^{-\Delta t/\tau} \quad (1)$$

Where Δt is the sampling interval. Then this parameter is used in the step function filer [7].

$$u_{k+1} = u_k + (v_{k+1} - v_0) e^{\Delta t/2\tau} - (v_k - v_0) e^{-\Delta t/2\tau} \quad (2)$$

Where v_0 : offset, v_k : voltage

3.1.2 Moving average filter

Secondly, the moving average filter is applied as it improves the signal to noise ratio. It reduces noise by filtering out high frequency data points which are largely deviating from the majority [14]. This is done by calculating the average number of points of the input signal within the data length L. This is then repeated for i points across the whole waveform. The equation is expressed as:

$$y[i] = \frac{1}{L} \sum_{j=0}^{L-1} x[i + j] \quad (3)$$

L represents the number of points averaged over. The resulting signal after in which the moving average filter has been implemented becomes smoother.

3.1.3 Differentiator

Finally, the steps involved in the differentiation filter is as follows:

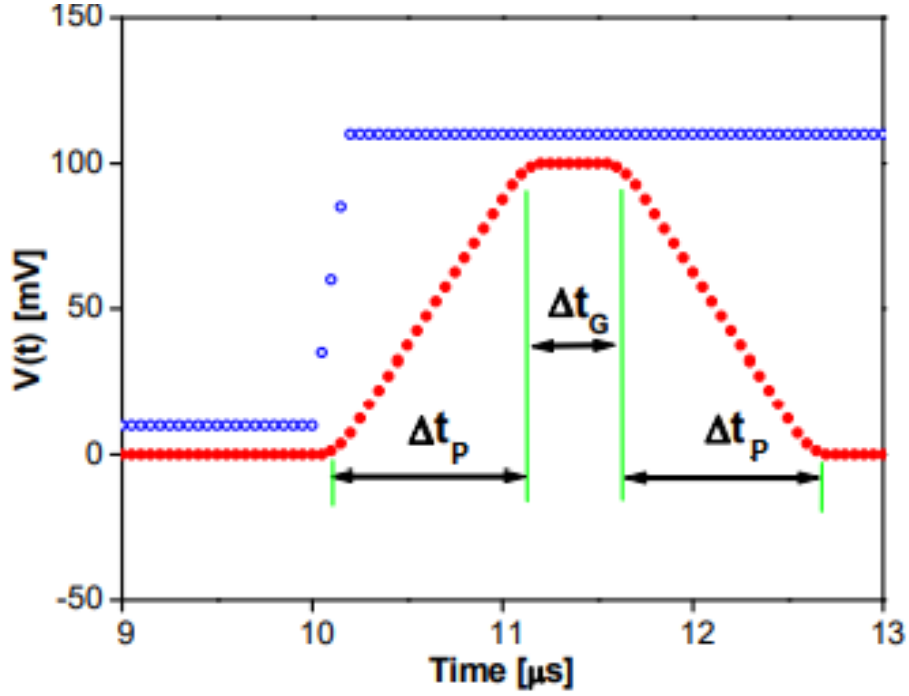


Figure 6: Image of the resulting trapezoid with respective parameters : peaking(P) and gap times(G). Image extracted from [14]

The three main steps of the trapezoidal filter is shown below [14]:

This computes the average value within P points repeated over i points:

$$V_{av1}[i] = \frac{1}{P} \sum_{j=0}^{P-1} V_{in}[i + j] \quad (4)$$

Compute the average again after a separation gap G for length P:

$$V_{av2}[i] = \frac{1}{P} \sum_{j=0}^{P-1} V_{in}[P + G + i + j] \quad (5)$$

The amplitude of the pulses are then taken by subtracting between two results above:

$$V_{out}[i] = V_{av2}[i] - V_{av1}[i] \quad (6)$$

The resulting shape is a trapezoid as shown in figure 6. The gap time(G) is the width of the flat top or simply the gap between the two peak times. The peaking time(P) represents the number of points which were taken for the trapezoidal algorithm to process.

3.2 Hardware

3.2.1 Digitizer

The digitizer has a sampling rate/interval of 4ns per channel/sample. A SIS3316 14 Channel VME Digitizer converts analog signal into a digital one. Input range of the digitizer is 2 volts and it has 16 channels with 14 bit data. It is connected to the HPGe detector.

3.2.2 Setup

The setup consists of several components. First of all, a radioactive ^{60}Co source that emits gamma rays is placed next to the high purity germanium detector(HPGe). The detector is then connected to the digitizer's input 1 which then is also connected to the computer. A delay was created by overlapping a pulse of a delay with 1,2,4 and 5 microseconds with the original pulse. A diagram is shown below:

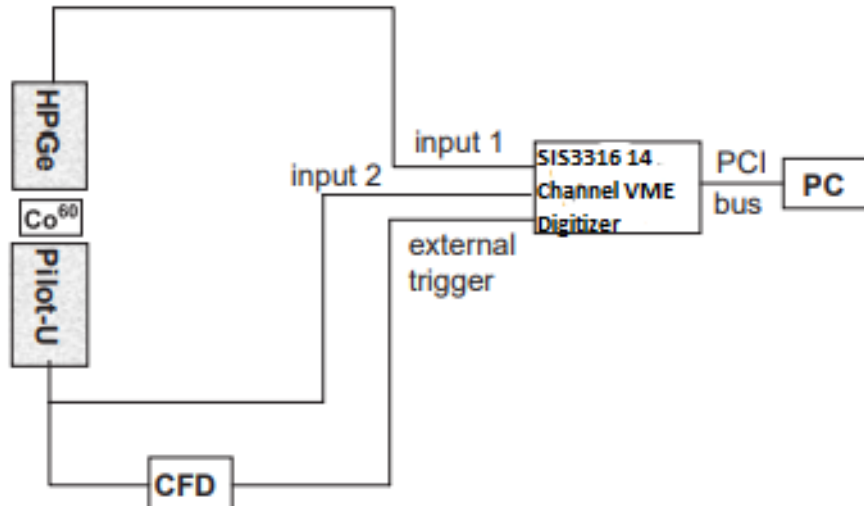


Figure 7: Setup diagram with ^{60}Co source. Image extracted from [7]

Each channel is 4 nano seconds apart and each waveform spans over 10000 channels.

3.3 Energy calibration

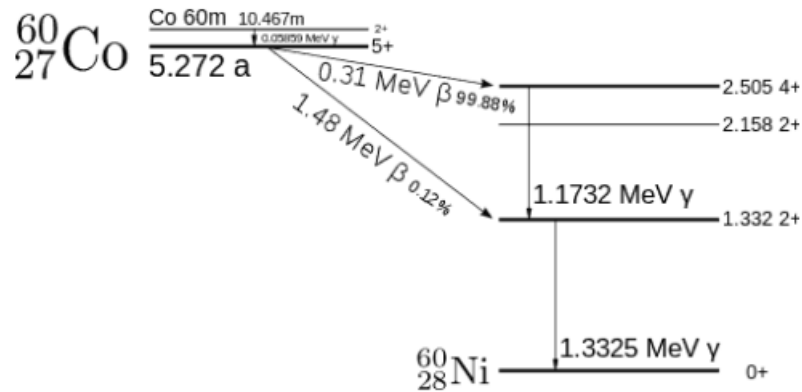


Figure 8: Decay scheme of ^{60}Co isotope. Image extracted from [15]

The figure above shows the decay scheme of the ^{60}Co isotope. Most of the time it will decay via beta emission to the excited state of ^{60}Ni which then is followed by a subsequent gamma decay to the ground state of 1.174 Mev or 1173.2 keV [15]. This is followed by a 1332.5 keV gamma emission to the ground state. Thus this would mean that there will be two photopeaks present in the energy spectrum: 1173.2 and 1332.5 keV. This report will be focusing on the 1173.3 keV peak. The full energy spectrum is shown below

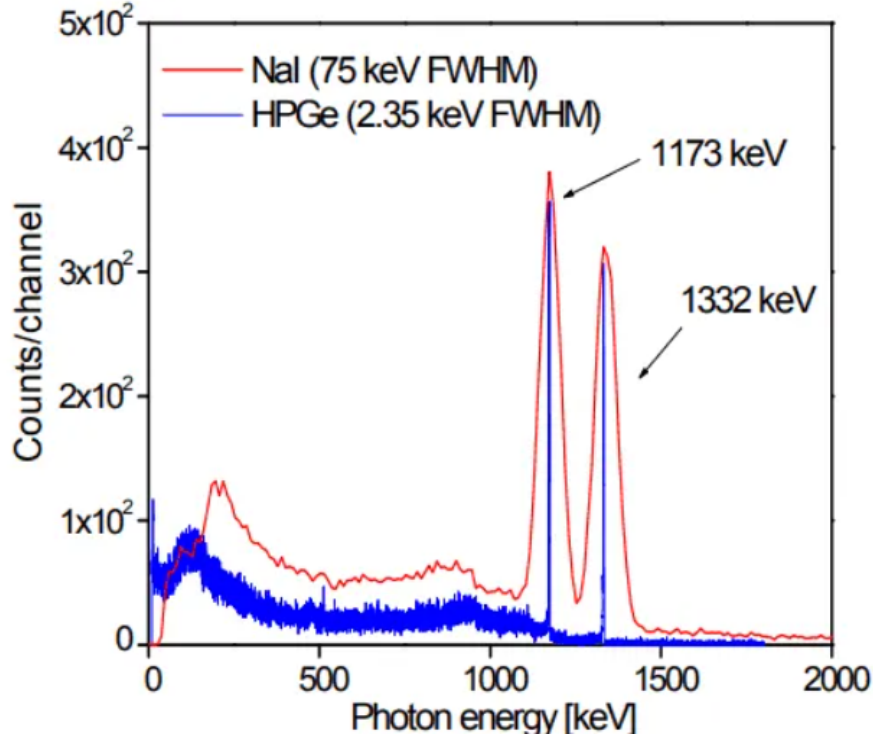


Figure 9: Energy spectrum of ^{60}Co using HPGGe detector. Image extracted from [15]

Once the spectrum is produced, the calibration is done by plotting the known energy peaks against the corresponding peak amplitudes with a linear relationship [16]. Using python's polyfit function, the parameters can be extracted [17]. This way the channels can be converted to energy. The equation is shown as follows:

$$E_{\gamma} = A + B \cdot \text{Peakamplitude} \quad (7)$$

3.4 Data Processing

Find the Optimal Peaking and gap values by varying the peak values in the range of 300 to 800 channels and gap values in the range of 130 to 200 channels. Plot the energy spectrum at the 1173.2 keV peak position and fit a gaussian Find the peak position in channels and calibrate channels to energy (keV) Plot the FWHM and mean energy (keV) against varying pulse time separation of 3000 to 6000 nanoseconds Compare the FWHM between with and without pulse pileup

Firstly, data which consisted of 111837 waveforms with each spanning over 5000 channels was provided to write an algorithm that accurately records the pulse amplitudes. After the algorithm has been written, the algorithm was tested by checking if it produces the correct energy spectrum for the real data collected from the Gelina facility(although it is not the exact same setup used).

Data were all processed and analyzed via Python using the Jupyter notebook. Once the data has been imported, the offset of the signal was found by finding the average of the signals before it starts rising. After that, using the raw data without the pileups, the method introduced in the algorithm section is implemented in its respective order, followed by the two peaks being recorded. This was done by first recording the first peak of the trapezoid(maximum value within waveform), then the minimum point of both the left or right side with respect to the first peak was recorded. The bigger value between either the left and right side was recorded.

The 1173.3 keV peak was then chosen. Since the peak position varies with the peaking and gap time, the optimal P and G values must first be extracted. The peak values in the range of 300 to 800 channels and gap values in the range of 130 to 200 channels were used and were plotted against the relative FWHM. The optimal P and G values are the values which corresponds to the lowest relative FWHM. Next, the peak position is then found for both the 1173.3 keV and 1332.5 keV peak to calibrate it. The FWHM (which is the width of the gaussian at half maximum) and mean energy(peak position), is plotted against the pulse time separation in the ranges of 3000, 4000, 5000, 6000 nanoseconds to see if the FWHM and mean energy changes or depends on the pulse time separation.

4 Results

All energy spectrums were generated via python to test if the algorithm can detect the two peaks of the pulse pile up. The 1173.3 keV peak was chosen, then fitted via gaussian using the curvefit function from scipy.optimize.

4.1 Optimizing P and G values

To accurately produce the energy spectrum of 60 co, it is required to find the optimal P and G values(in channels). This was done by plotting the relative FWHM(in channels/amplitude) against different peaking and gap times. The optimal peaking and gap time is when its value corresponds to the lowest FWHM as it implies it has a narrower resolution. The plot is shown below.

The standard deviation was calculated by using scipy.stats.norm. This was used to calculate the full width at half maximum. Full width at half maximum is calculated as $FWHM = 2\sqrt{2\log 2} \times \sigma$ where sigma is the standard deviation [18].

The plot of the relative FWHM against the P and G values are shown below:

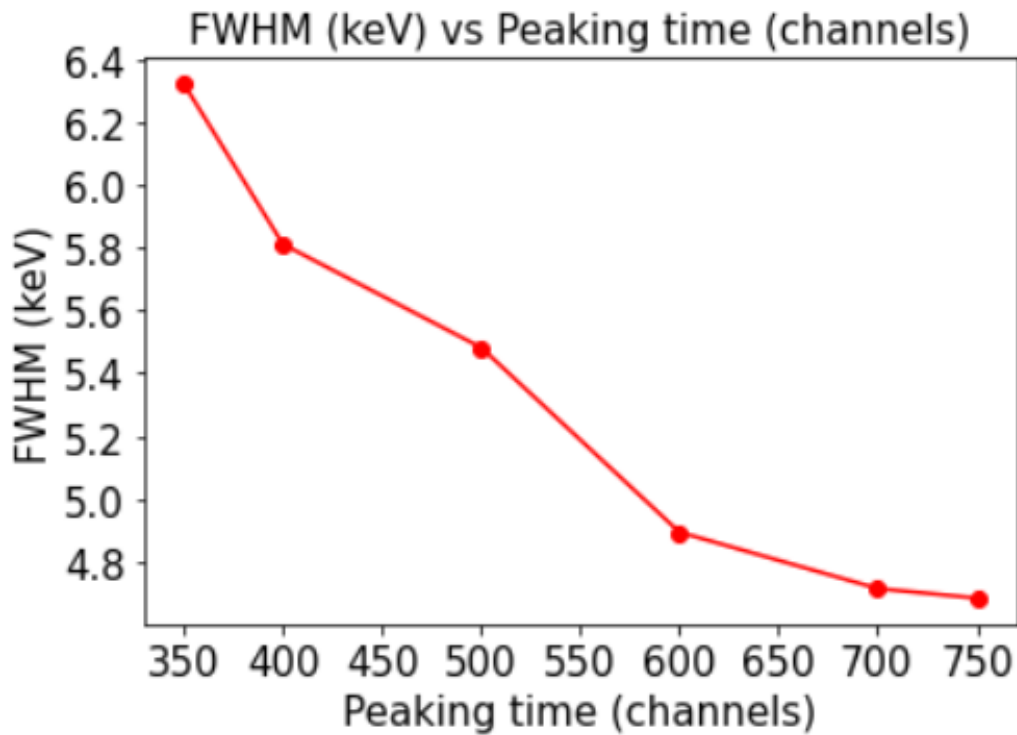


Figure 10: Above: The plot of FWHM against varying Peaking time(constant G = 130) around the 1173.2 keV peak.

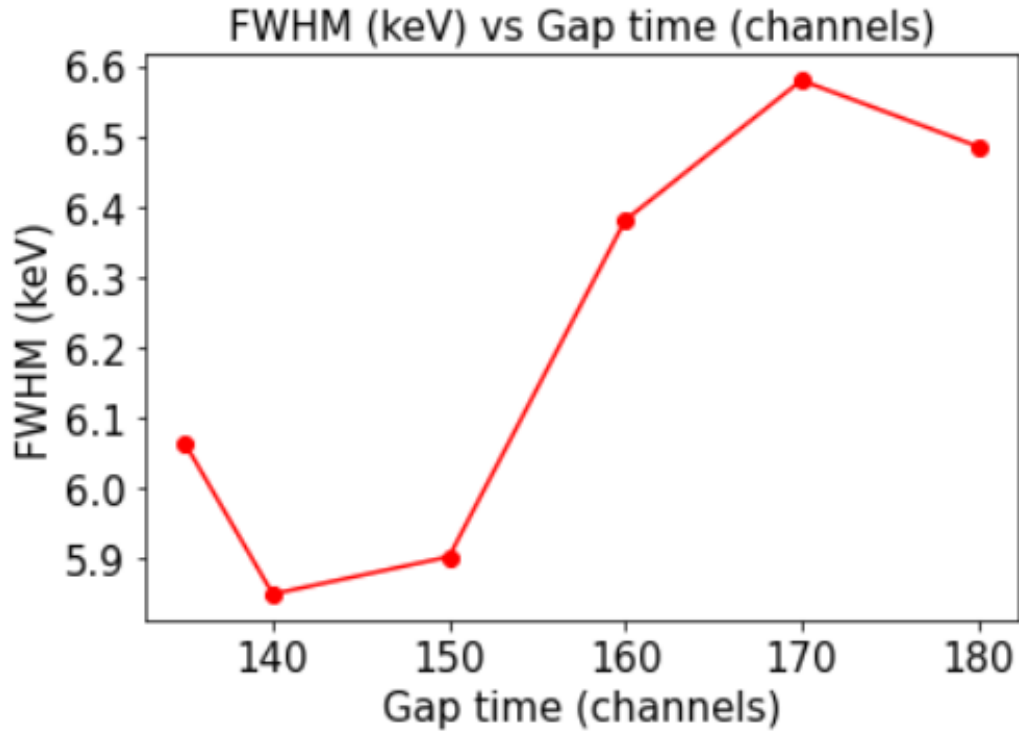


Figure 11: Above: The plot of FWHM against varying gap time(constant $P = 400$) around the 1173.2 keV peak.

It is observed that the FWHM is the smallest when $P = 750$ and $G = 140$, implying that it has the most narrow resolution at this configuration.

4.2 Energy calibration

In order to convert the amplitude to the energy, a calibration must be done. First a gaussian is fitted for both peaks on the spectrum: 1173.2 keV and 1332.5 keV. After that, the peak positions(in amplitude/channels) of the two known gaussian peaks are plotted against the known energy values which are 1173.2 keV and 1332.5 keV assuming that the relationship between the two are linear. This was done via the poly.fit function in python. The extracted values are: gradient = 0.65 and the y intercept = 0.72. This way the x-axis can all be converted to units in keV.

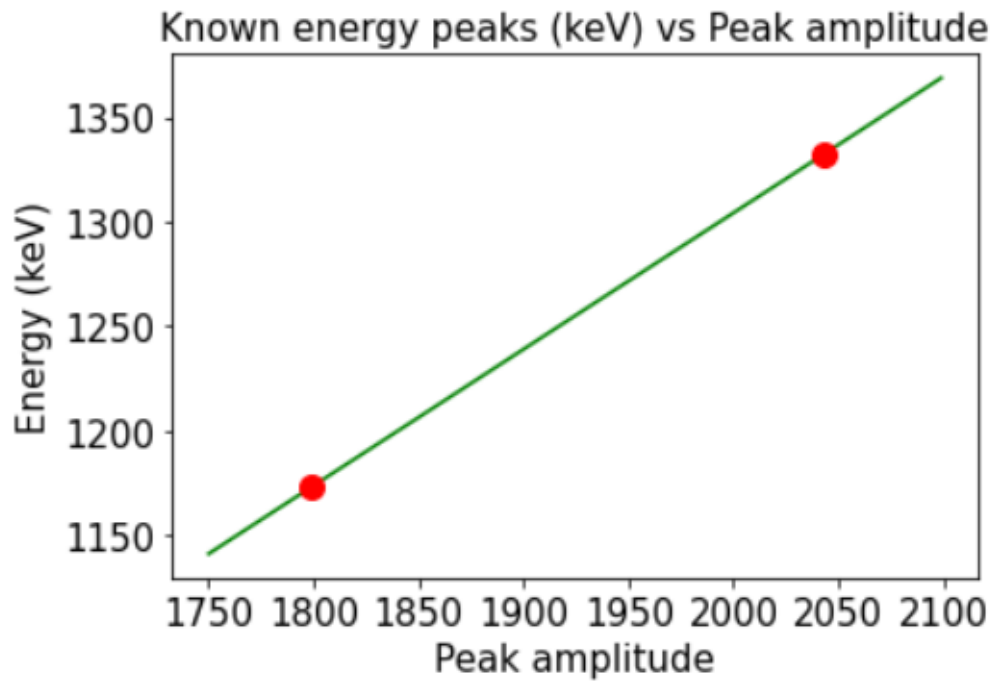


Figure 12: The calibration function. Their peak positions are plotted to the corresponding known energy values of the ^{60}Co peaks.

The energy spectrum at the 1173.5 keV peak with $P = 750$ and $G = 140$ is shown below:

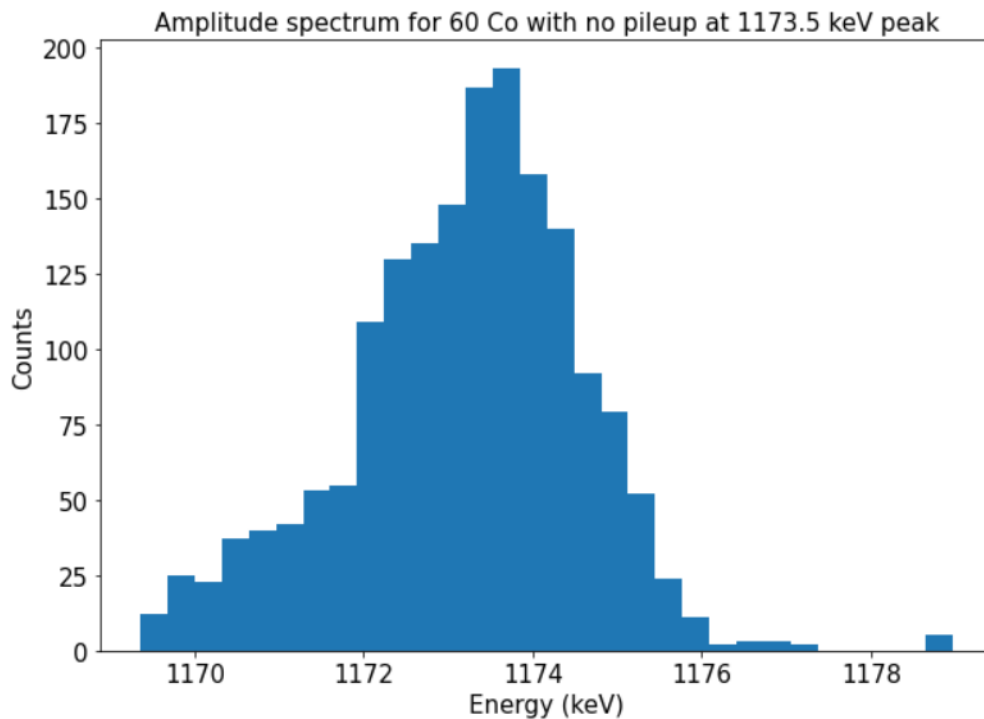


Figure 13: The amplitude spectrum of the ^{60}Co source around the 1173.2 keV peak with no pileups with 20000 waveforms

The full calibrated energy spectrum is shown below:

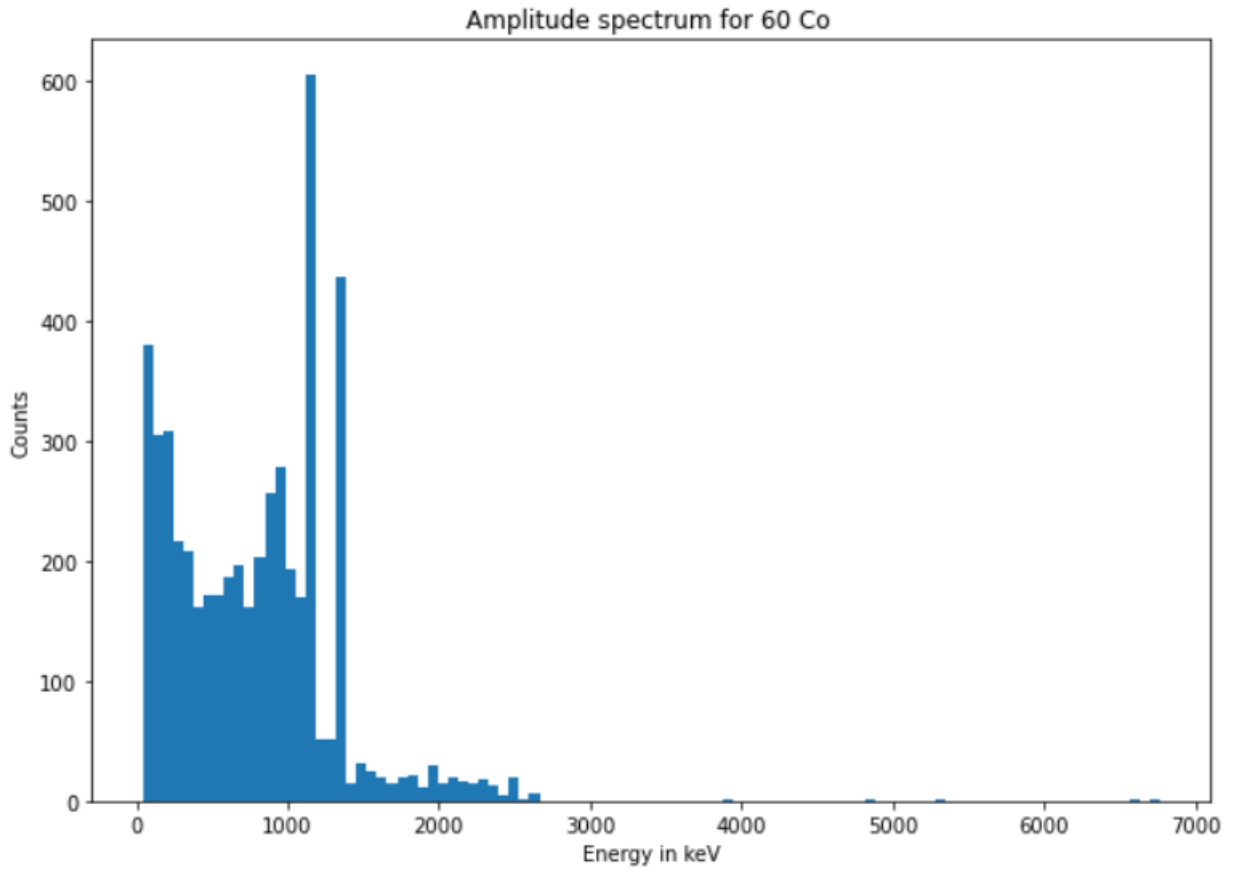


Figure 14: The energy spectrum of the ^{60}Co source

4.3 Relationship between mean energy/FWHM and pulse pileup delay

After figuring out the optimal values for the peaking and gap time, the mean energy was plotted against the pulse pileup delay to check if the algorithm has accurately recorded the peaks at its correct value with the presence of the pulse pileup. The plot is shown below:

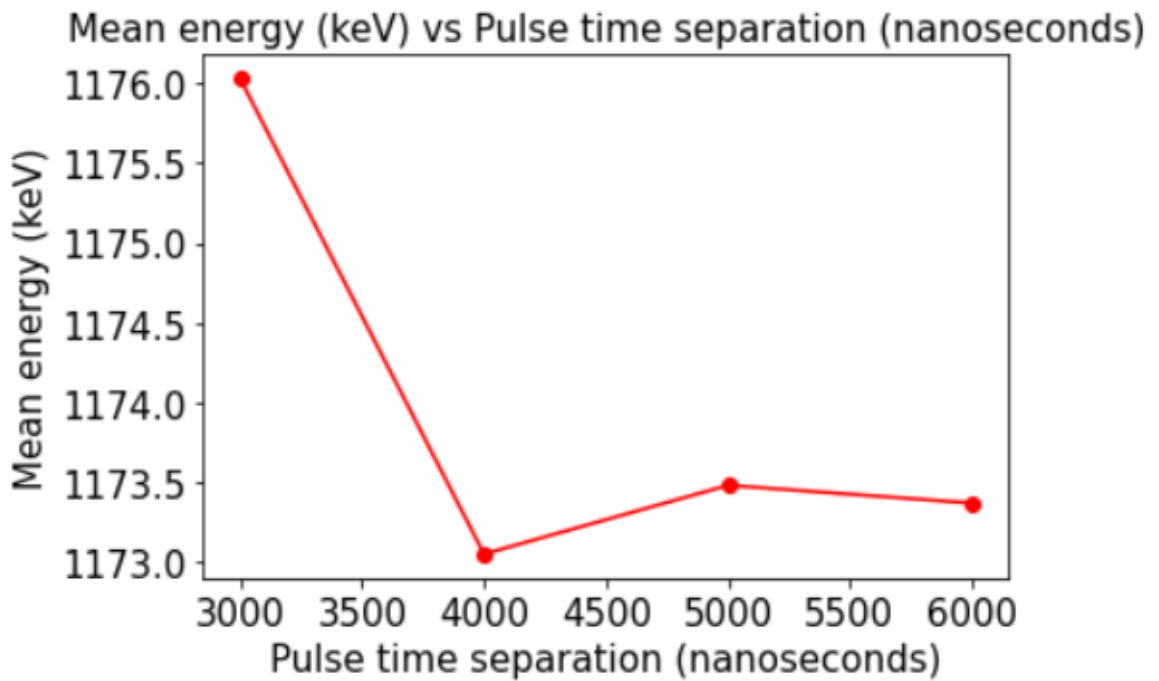


Figure 15: The mean energy(keV) against pulse time separation (nanoseconds).

It is observed that the mean energy starts to fluctuate largely when the pulse time separation is below 4000 nanoseconds.

The FWHM against the pulse time separation is shown below:

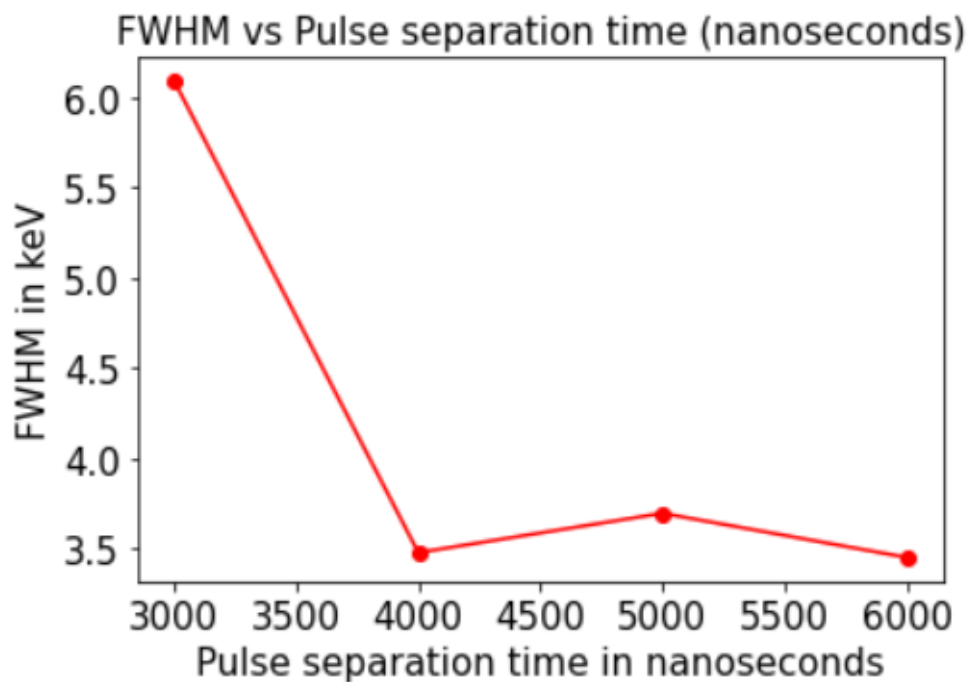


Figure 16: The FWHM(keV) against pulse time separation (nanoseconds).

As observed, the resolution starts to suffer below 4000 nanoseconds.

The average full width at half maximum(FWHM) between 4000 to 6000 nanoseconds of pulse time separation is 3.54 keV. It then drastically increases to above 6.0 keV. The energy spectrum at the 1173.3 keV peak with 6000 nanoseconds of pulse time separation is shown below:

Energy spectrum for 60 Co with 6000 nanoseconds pulse time separation at 1173.5 keV peak

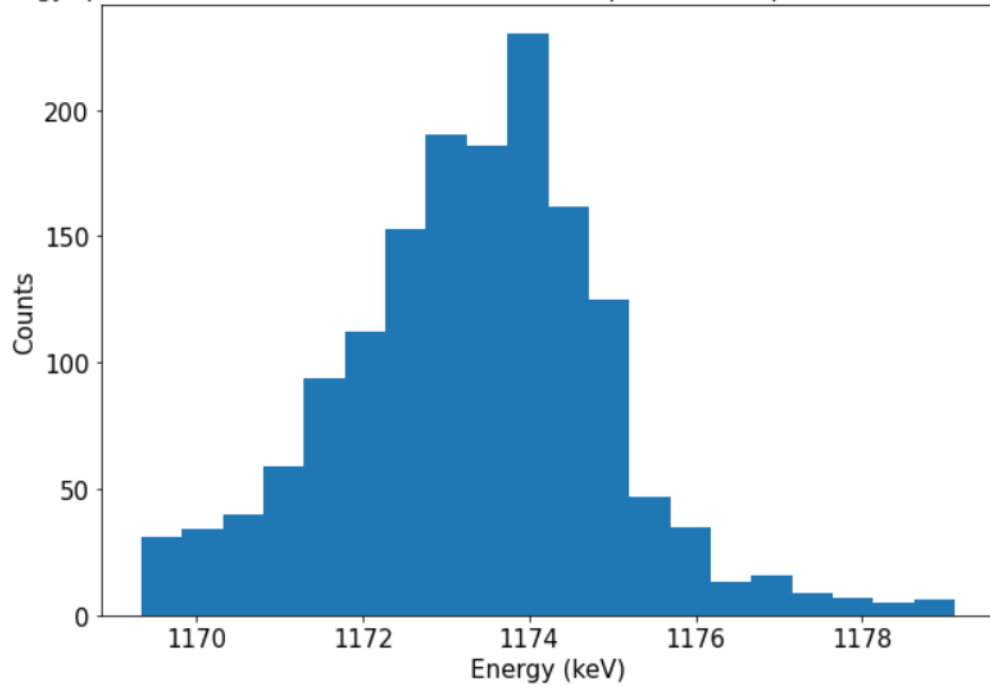


Figure 17: The amplitude/energy spectrum of the 60Co source around the 1173.2 keV peak with pulse time separation of 6000 nanoseconds.

As evident from the figure above, the energy spectrum at around the 1173.3 keV peak with 6000 nanoseconds of pulse time separation almost resembles with the energy spectrum without pileups implying that the energy spectrum is not that distorted. The FWHM with 6000 nanoseconds is 3.45 keV.

5 Discussion

There are several limitations in this method. First of all, the most obvious limitation of this methodology is that it only works for pulses with two pileups. In reality pulse pileups can be more than 2, thus this method has little to no practicality. But if modified, this algorithm could detect three pulses if not just either the left or right pulse is recorded, but both are as long as they are above the energy threshold of the HPGe detector.

Secondly, the theoretical value at which the pulse pileup can be distinguished should be approximately 2.5 microseconds, however as shown in the results section, the mean energy starts to increase when the pulse separation goes below 4 microseconds. This happens when the trapezoidal algorithm not being able to distinguish between the two pulses. This may have been caused by flaws in the trapezoidal algorithm. The data is usually analyzed using the room program, thus limited literature is available for python algorithms. But since these literature values were obtained using better equipment and in ideal conditions, it may not be a viable comparison as the scale of the experiment is much smaller in this project.

Finally, due to limitations of computing power, larger ranges of pulse time separations were not possible to plot against the mean energy and FWHM. Thus if one were to repeat or improve this investigation, python is not advised as there are other programs which are designed to analyze this. Also a computer with larger RAM is ideal as only 20000 waveforms were considered to construct the spectrum as it is time consuming.

5.1 Energy resolution

The average FWHM without pulse pileups is 3.26 keV compared to with pulse pileups which is 3.54 keV. This may be caused by the fact that the baseline restoration was not done, thus pulses with higher offsets and existing pileups in the raw data were not omitted. This possibly led to the values of the amplitudes recorded to fluctuate causing random errors between the data which includes pulse pileups and the other which does not include pileups.

5.2 Peaking and gap time

The optimal peaking time (750 channels) ended up inclining towards the largest possible P value(800 channels). This also may have led to the minimum pulse time separation that can be distinguished in the trapezoidal algorithm to increase. Increasing the peaking and gap time increases the pulse width, thus making it more susceptible to pulse pileups which are harder to distinguish. This can lead to distortions in the energy spectrum such as leading to larger values of FWHM as the trapezoidal filter detects them as one pulse. Larger peaking and gap time values also reduces the range at which the pulse pileups can be distinguished as two separate pulses. As expected, the ranges at which the trapezoidal filtering can detect two pulses in a situation where pileups occur decreased.

5.3 Energy calibration

Another limitation of this project was that it only uses ^{60}Co as a calibration source, leading to vague linear representations of the relationship between the energy in keV and the peak centre. Ideally, using multiple photon/radioactive sources with various photopeaks such as ^{134}Cs would be desired as more points can be included in the linear relationship while calibrating, thus a more accurate linear relationship can be extracted [16]. That way the parameters of the linear expression will be more accurate.

6 Conclusion

As a conclusion, through trapezoidal filtering, it is possible to detect the energy of two pulses when piled up together. The signal had to undergo a series of corrections to account for: ballistic deficits, pulse pile up and noise reduction. These were done using the step filter function, trapezoidal filter and moving average filter respectively. The data included 111837 waveforms with each waveform spanning 5000 channels where each channel spans 4 nanoseconds. In order to investigate the effects of pileups, it was required to artificially construct pileups by adding the signals together with varying pulse time separations between 3000 to 6000 microseconds. The FWHM without pileups is found to be 3.26 keV, whereas the FWHM is 3.54 keV without pileups. From the data extracted, a minimum of 4000 nanoseconds of pulse time separation is required for the pulse separation in order to accurately measure its energy without distortion of its spectrum. The optimal value of the P and G values are known to be $P = 750$ and $G = 140$.

References

- [1] Martina Igini. *The Advantages and Disadvantages of Nuclear Energy*. EARTH.ORG. URL: <https://earth.org/the-advantages-and-disadvantages-of-nuclear-energy/>.
- [2] Nuclear Energy Insitute. *Comparing Fukushima and Chernobyl*. Nuclear Energy Insitute.
- [3] Jennifer A. Shusterman et al. “The surprisingly large neutron capture cross-section of ^{88}Zr ”. In: *Nature* 565.7739 (2019), pp. 328–330. ISSN: 0028-0836. DOI: 10.1038/s41586-018-0838-z.
- [4] Leo Williams. *What makes neutron scattering unique*. Oak Ridge National Library. URL: <https://www.ornl.gov/blog/what-makes-neutron-scattering-unique>.
- [5] Nick Connor. *What is application of hpge detectors - definition*. Dec. 2019. URL: <https://www.radiation-dosimetry.org/what-is-application-of-hpge-detectors-definition/>.
- [6] Nick Connor. *What is high purity germanium detector - hpge - definition*. Dec. 2019. URL: <https://www.radiation-dosimetry.org/what-is-high-purity-germanium-detector-hpge-definition/>.
- [7] L.C. Mihailescu, C. Borcea, and A.J.M. Plompen. “Data acquisition with a fast digitizer for large volume hpge detectors”. In: *Nuclear Instruments and Methods in Physics Research Section A: Accelerators, Spectrometers, Detectors and Associated Equipment* 578.1 (2007), pp. 298–305. DOI: 10.1016/j.nima.2007.05.231.
- [8] *Bremsstrahlung*. URL: <https://www.britannica.com/science/bremsstrahlung>.
- [9] M. Flaska et al. “Modeling of the gelina neutron target using coupled electron–photon–neutron transport with the MCNP4C3 code”. In: *Nuclear Instruments and Methods in Physics Research Section A: Accelerators, Spectrometers, Detectors and Associated Equipment* 531.3 (2004), pp. 392–406. DOI: 10.1016/j.nima.2004.05.087.
- [10] M. Kerveno et al. “From γ emissions to (n,xn) cross sections of interest: The role of GAINS and GRAPHEME in nuclear reaction modeling”. In: *The European Physical Journal A* 51.12 (2015). ISSN: 1434-6001. DOI: 10.1140/epja/i2015-15167-y.
- [11] *Pulse Pile-up and Pile-up Rejection*. Radiation Solutions Inc. URL: https://www.radiationsolutions.ca/fileadmin/pdf/Pulse_Pile-up.pdf.
- [12] B.W. Loo, F.S. Goulding, and D. Gao. “Ballistic deficits in pulse shaping amplifiers”. In: *IEEE Transactions on Nuclear Science* 35.1 (1988), pp. 114–118. ISSN: 0018-9499. DOI: 10.1109/23.12686. URL: <https://dx.doi.org/10.1109/23.12686>.
- [13] Zbigniew Guzik and Tomasz Krakowski. “Algorithms for digital -ray spectroscopy”. In: *Nukleonika* 58 (Jan. 2013), pp. 333–338.
- [14] Soo Hyun Byun. *Med Phys 4RA3, 4RB3 6R03 Radioisotopes and Radiation Methodology I, II*. 2019-2020.

- [15] *Cobalt-60 spectrum*. June 2022. URL: <https://www.nuclear-power.com/nuclear-engineering/radiation-detection/gamma-spectroscopy/cobalt-60-spectrum/>.
- [16] Aurelian Luca et al. “Calibration of the high and low resolution gamma-ray spectrometers”. In: *Romanian Reports in Physics* 64 (Jan. 2012), pp. 968–976.
- [17] *Numpy.polyfit*. URL: <https://numpy.org/doc/stable/reference/generated/numpy.polyfit.html>.
- [18] *Full width at half maximum*. URL: <https://mathworld.wolfram.com/FullWidthatHalfMaximum.html>.

7 Appendix

7.1 FWHM and mean energy against pulse time separation values

Pulse time separation(<i>ns</i>)	3000	4000	5000	6000
FWHM (keV)	6.09	3.48	3.70	3.45
Mean energy (keV)	1176.03	1173.05	1173.48	1173.37

Table 1: FWHM and Mean values (keV) against the pulse time separation (nanoseconds)